SUPPLEMENTAL DATA

Figure S1.

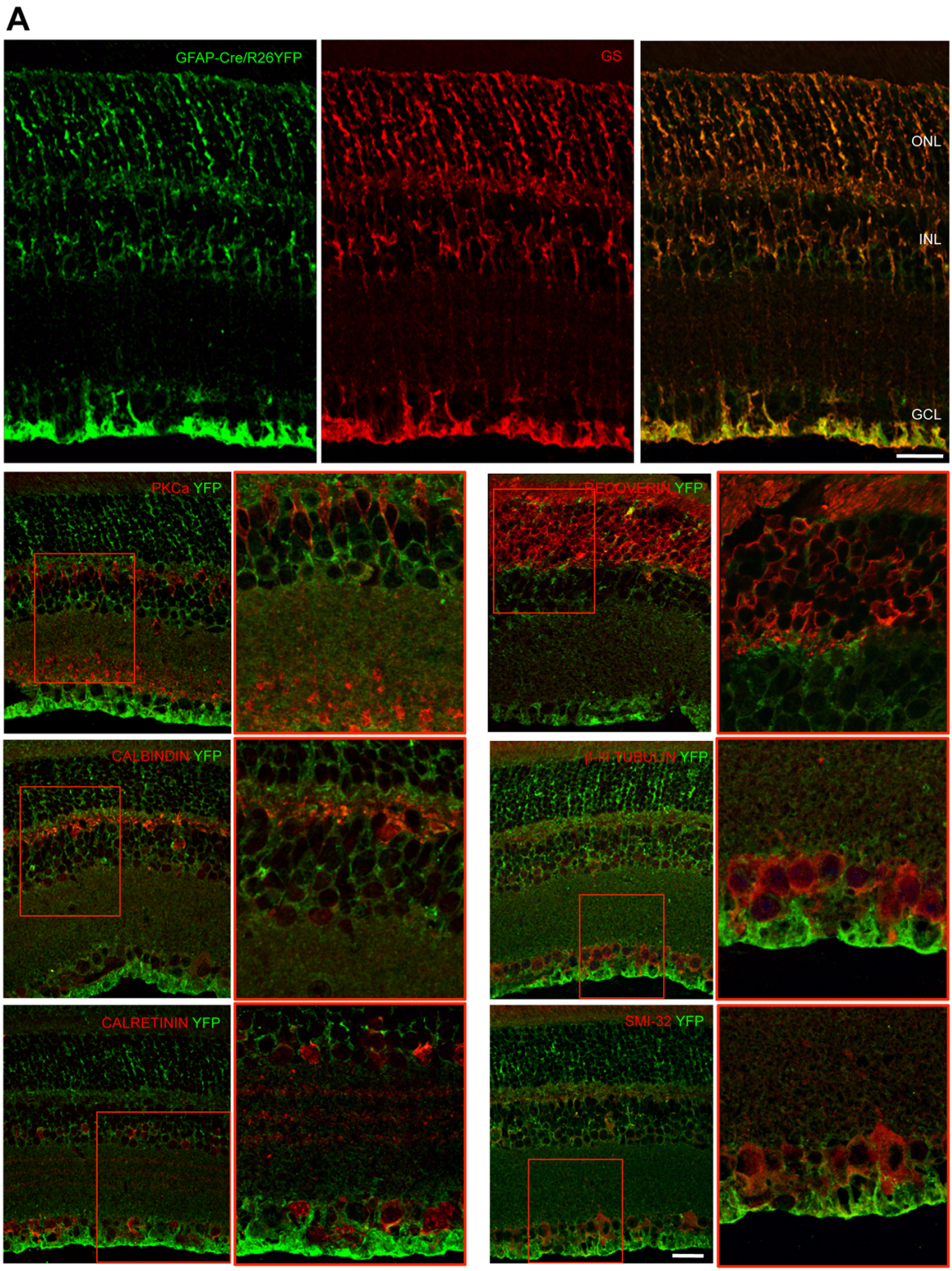

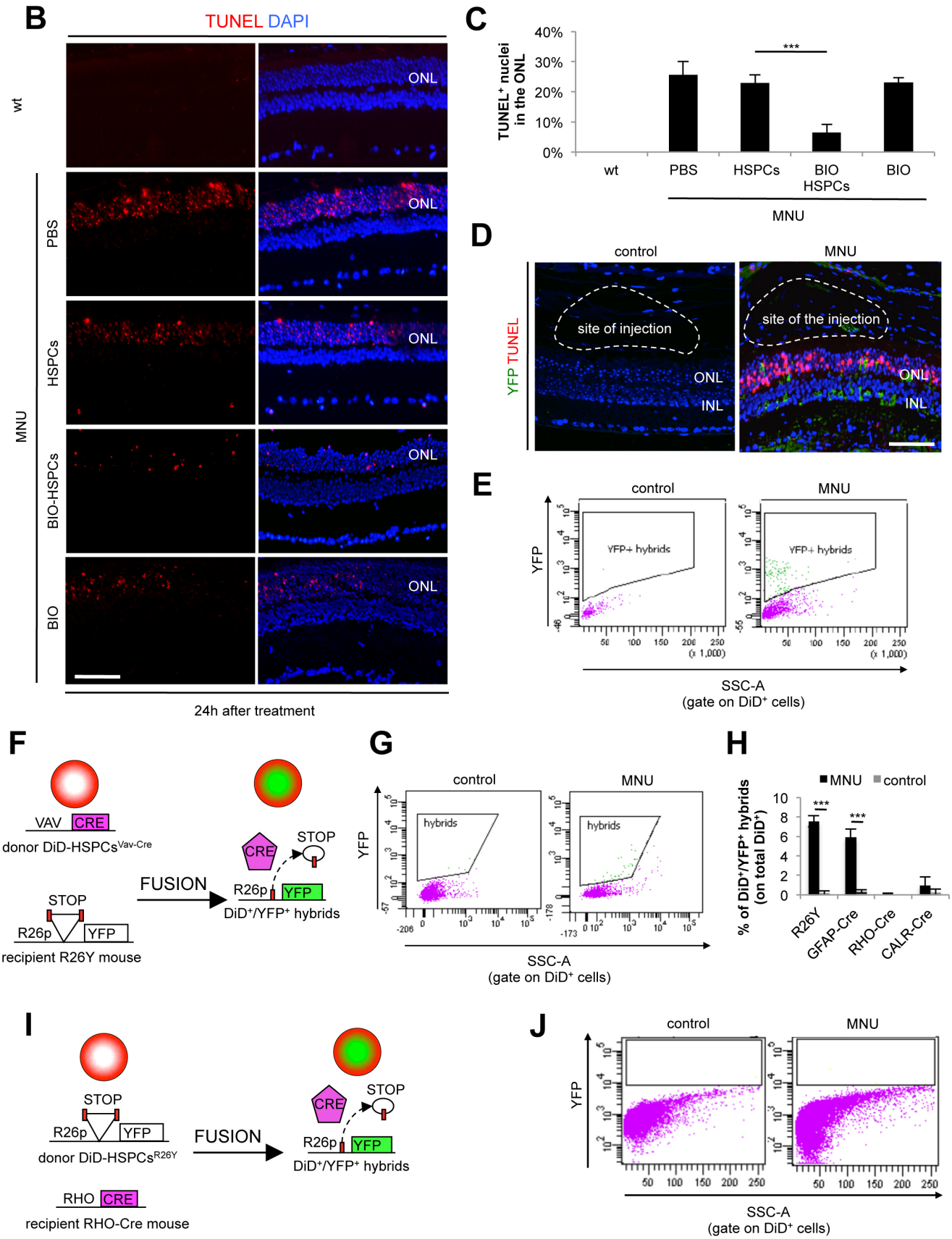
B
TUNEL DAPI
wt
MNU
PBS
HSPCs
BIO-HSPCs
BIO
ONL
24h after treatment
C
TUNEL+ nuclei in the ONL
40%
30%
20%
10%
0%
***
wt
PBS
HSPCs
BIO HSPCs
BIO
MNU
D
control
MNU
YFP TUNEL
site of injection
site of the injection
ONL
INL
E
control
MNU
YFP
YFP+ hybrids
SSC-A
(gate on DiD+ cells)
F
VAV CRE
donor DiD-HSPCsVav-Cre
STOP
R26p YFP
recipient R26Y mouse
FUSION
CRE
STOP
R26p YFP
DiD+/YFP+ hybrids
G
control
MNU
YFP
hybrids
SSC-A
(gate on DiD+ cells)
H
MNU
control
% of DiD+/YFP+ hybrids (on total DiD+)
***
R26Y
GFAP-Cre
RHO-Cre
CALR-Cre
I
STOP
R26p YFP
donor DiD-HSPCsR26Y
RHO CRE
recipient RHO-Cre mouse
FUSION
CRE
STOP
R26p YFP
DiD+/YFP+ hybrids
J
control
MNU
YFP
SSC-A
(gate on DiD+ cells)

Figure S1. Cell fusion of transplanted HSPCs with MG

(**A**) Representative double immunostainings of YFP (green) and different markers specific for either Müller glia (GS, red), bipolar cells (PKCa, red), horizontal cells (CALBINDIN, red), amacrine and ganglion cells (CALRETININ, red), photoreceptors (RECOVERIN, red), or ganglion cells (β-III-TUBULIN and SMI-32, red) in GFAP-Cre/R26YFP retinas obtained by crossing a transgenic mouse strain carrying the Cre-recombinase driven by the GFAP promoter with R26YFP reporter mice. ONL: outer nuclear layer; INL: inner nuclear layer; GCL: ganglion cell layer. Scale bar: 20 μm. (n=3). (**B**) Detection of $TUNEL^+$ (red) apoptotic photoreceptors in the ONL of healthy (wt) or MNU-damaged (MNU) retinas 24 h after treatment with either vehicle (PBS), HSPCs (HSPCs), BIO-treated HSPCs (BIO-HSPCs), or BIO alone (BIO) as control. Nuclei were counterstained with DAPI (blue). ONL: outer nuclear layer. Scale bar: 20 μm. (**C**) Statistical analysis of the percentages of apoptotic photoreceptors evaluated as the number of $TUNEL^+$ nuclei with respect to the total amount of nuclei in the ONL counted in retinal sections from healthy (wt) or MNU-damaged (MNU) eyes treated with either vehicle (PBS), HSPCs (HSPCs), BIO-treated HSPCs (BIO-HSPCs), or BIO alone (BIO) as control. Bars represent means ±S.D. from 3 independent experiments (n=9). ***P-value <0.0001 by unpaired Students' t-test. (**D**) Representative immunostaining of YFP^+ hybrids (green) and $TUNEL^+$ (red) apoptotic photoreceptors in retinal sections harvested from MNU-damaged (MNU) or healthy (control) GFAP-Cre eyes 12 h after sub-retinal transplantation of $HSPCs^{R26Y}$. YFP^+ hybrids (green) derived from cell fusion are detected close to the site of the injection (dashed lines) in MNU-damaged (MNU) retinas but not in the undamaged eyes (control). No major changes in the retinal morphology were detected upon sub-retinal injection. Nuclei were counterstained with DAPI (blue). The image represents a picture of the same region shown in Figure 1B. ONL: outer nuclear layer. INL: inner nuclear layer. Scale bar: 200 μm. (n=3). (**E**) Representative FACS analysis of DiD^+/YFP^+ hybrids in the total DiD^+ population detected in healthy (control) or MNU-damaged (MNU) GFAP-Cre retinas harvested 24 h after transplantation of DiD-labeled $HSPCs^{R26Y}$. (n=3). (**F**) Schematic representation of the cell fusion detection in the R26Y mouse model. Cell fusion between DiD-labeled HSPCs isolated from Vav-Cre transgenic mice (DiD-$HSPCs^{Vav\text{-}Cre}$) and recipient R26Y retinal cells leads to the formation of DiD^+/YFP^+ hybrids. (**G**) Representative FACS analysis of DiD^+/YFP^+ hybrids in the total DiD^+ population detected in MNU-damaged (MNU) or healthy (control) R26Y retinas harvested 24 h after transplantation of DiD-$HSPCs^{Vav\text{-}Cre}$. (n=3). (**H**) Percentages of double DiD^+/YFP^+ hybrids on the total DiD^+ population detected by FACS analysis of healthy (control, gray bars) or MNU-damaged (MNU, black bars) R26Y (R26Y), GFAP-Cre (GFAP), Rhodopsin-Cre (RHO-Cre) or Calretinin-Cre (CALR- Cre) retinas 24 h after transplantation of $HSPCs^{Vav\text{-}Cre}$ or $HSPCs^{R26Y}$. Data are means ±S.D. from three independent experiments (n=3). ***P-value <0.0001 by unpaired Students' t-test. (**I**) Schematic representation of the experimental plan to detect fusion with photoreceptors. Cell fusion between HSPCs isolated from R26Y donor mice ($HSPCs^{R26Y}$) and recipient RHO-Cre photoreceptors leads to the possible formation of YFP^+ hybrids. (**J**) Representative FACS analysis of DiD^+/YFP^+ hybrids in the total DiD^+ population detected in MNU-damaged (MNU) or healthy (control) RHO-Cre retinas harvested 24 h after transplantation of DiD-$HSPCs^{R26Y}$. (n=3).

Figure S2.

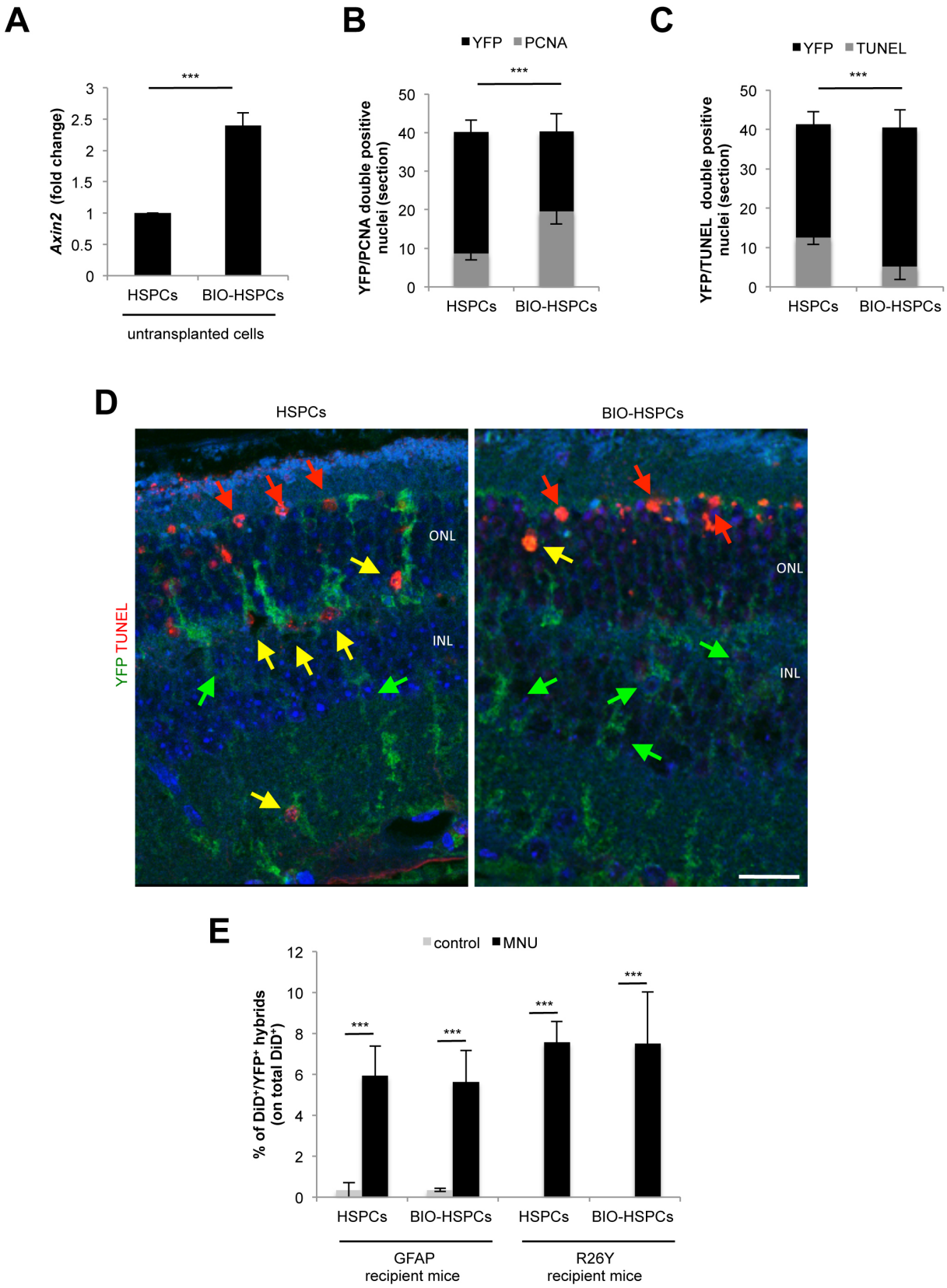
A
Axin2 (fold change)
***
HSPCs
BIO-HSPCs
untransplanted cells
B
YFP PCNA
YFP/PCNA double positive nuclei (section)
***
HSPCs
BIO-HSPCs
C
YFP TUNEL
YFP/TUNEL double positive nuclei (section)
***
HSPCs
BIO-HSPCs
D
HSPCs
BIO-HSPCs
YFP TUNEL
ONL
INL
E
control MNU
% of DiD+/YFP+ hybrids (on total DiD+)
***
HSPCs
BIO-HSPCs
GFAP recipient mice
R26Y recipient mice

Figure S2. Proliferation and apoptosis of hybrids in transplanted retinas.
(**A**) RT-PCR quantification of *Axin2* (Wnt/β-catenin target gene) expression in HSPCs treated with 1 μM BIO for 24 h (BIO-HSPCs) with respect to untreated control HSPCs (HSPCs). BIO is a GSK3 inhibitor and is used to activate the Wnt/β-catenin pathway (63). Data are means ±S.D. from 3 independent experiments (n=3). ***P-value <0.0001 by unpaired Students' t-test. (**B, C**) Statistical analysis of the total number of YFP^+ hybrids (black bars) also positive for either PCNA (gray bars in B) or for TUNEL (gray bars in C) detected in retinal sections harvested from MNU-damaged GFAP-Cre retinas 24 h after transplantation of untreated (HSPCs) or BIO-treated (BIO-HSPCs) $HSPCs^{R26Y}$. Data are means ±S.D. from 3 independent experiments (n=9). ***P-value <0.0001 by unpaired Students' t-test. (**D**) Representative confocal images of YFP-positive hybrids (green) and TUNEL-positive cells (red) in MNU-damaged GFAP-Cre retinas 24 h after transplantation of BIO-treated (BIO-HSPCs) or untreated (HSPCs) $HSPCs^{R26Y}$. Yellow arrows show YFP^+ hybrids that undergo apoptosis ($TUNEL^+$). Green arrows show YFP^+ hybrids that do not undergo apoptosis ($TUNEL^-$). Red arrows show $YFP^-/TUNEL^+$ photoreceptors in the ONL that undergo apoptosis. Nuclei were counter stained with DAPI (blue). Scale bar: 20 μm. (**E**) Percentages of double DiD^+/YFP^+ hybrids on the total DiD^+ population detected by FACS analysis of healthy (control) or MNU-damaged (MNU) GFAP-Cre (GFAP recipient mice) and R26Y (R26Y recipient mice) retinas 24 h after transplantation of either untreated (HSPCs, grey bars) or BIO-treated (BIO-HSPCs, black bars) $HSPCs^{R26Y}$ or $HSPCs^{Vav\text{-}Cre}$, respectively. Data are means ±S.D. from 3 independent experiments (n=3). Data relative to HSPC transplantation in GFAP-Cre mice are the same included in Figure 1C. ***P-value <0.0001 by unpaired Students' t-test.

Figure S3.

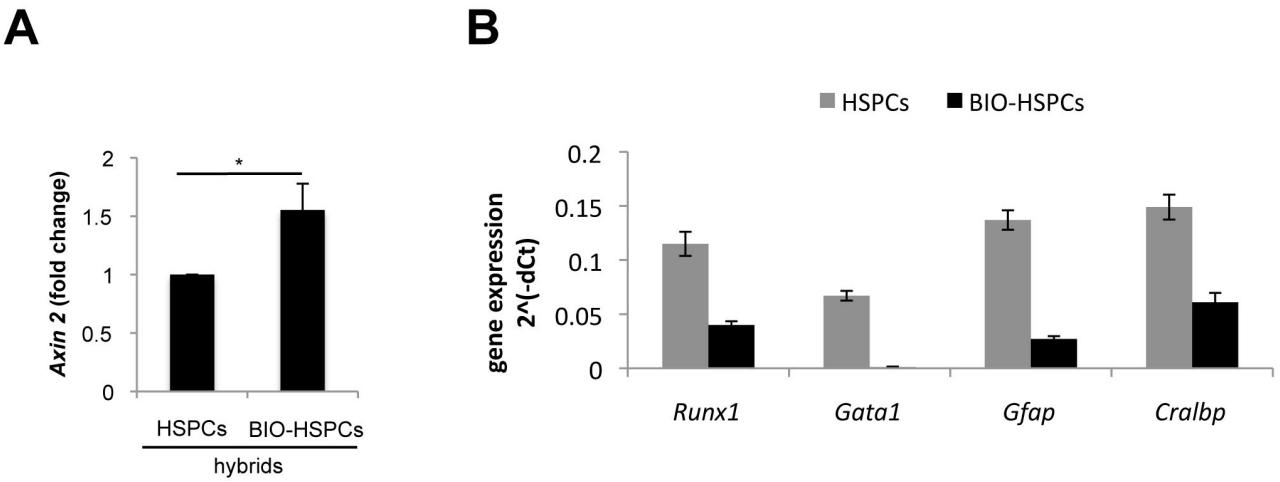

Figure S3. Gene expression of differentiation genes and Wnt pathway activation in hybrids.

(**A**) RT-PCR quantification of *Axin2* expression in YFP^+/DiD^+ hybrids FACS sorted from MNU-damaged GFAP-Cre retinas 24 h after transplantation of DiD-labelled BIO-treated (BIO-HSPCs) or untreated (HSPCs) $HSPCs^{R26Y}$. Data are the means ±S.D. of the fold-changes of Axin2 expression in hybrids obtained upon fusion with BIO-HSPCs with respect to hybrids obtained upon fusion with HSPCs (n=3). *P-value <0.01 by unpaired Students' t-test. (**B**) Gene expression levels in DiD^+/YFP^+ hybrids sorted 24 h after transplantation of untreated (HSPCs, gray bars) or BIO-treated (BIO-HSPCs, black bars) $HSPCs^{R26Y}$ in MNU-damaged GFAP-Cre recipient eyes. Data are means ±S.D. from 3 independent experiments (n=3).

Figure S4.

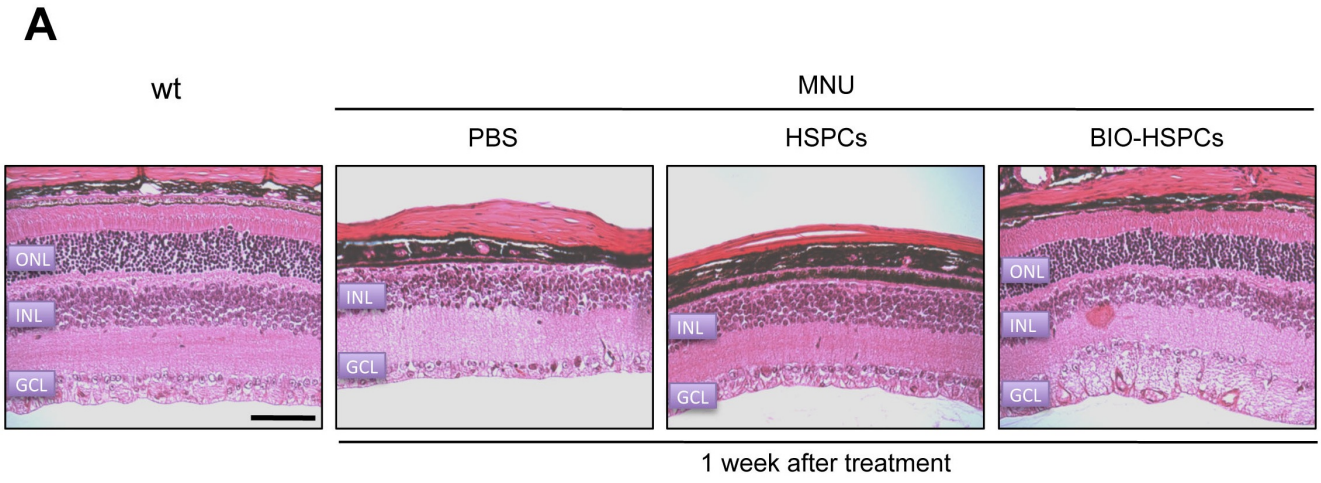

Figure S4. Analysis of photoreceptor cell death in MNU-damaged eyes.
(A) Representative hematoxylin and eosin staining of retinal sections of the area close to the site of the injection from healthy (wt) or MNU-damaged (MNU) eyes 1 week after transplantation with either vehicle alone (PBS), untreated (HSPCs) or BIO-treated HSPCs (BIO-HSPCs). ONL: outer nuclear layer; INL: inner nuclear layer; GCL: ganglion cell layer. Scale bar: 200 μm. (n=3).

Figure S5

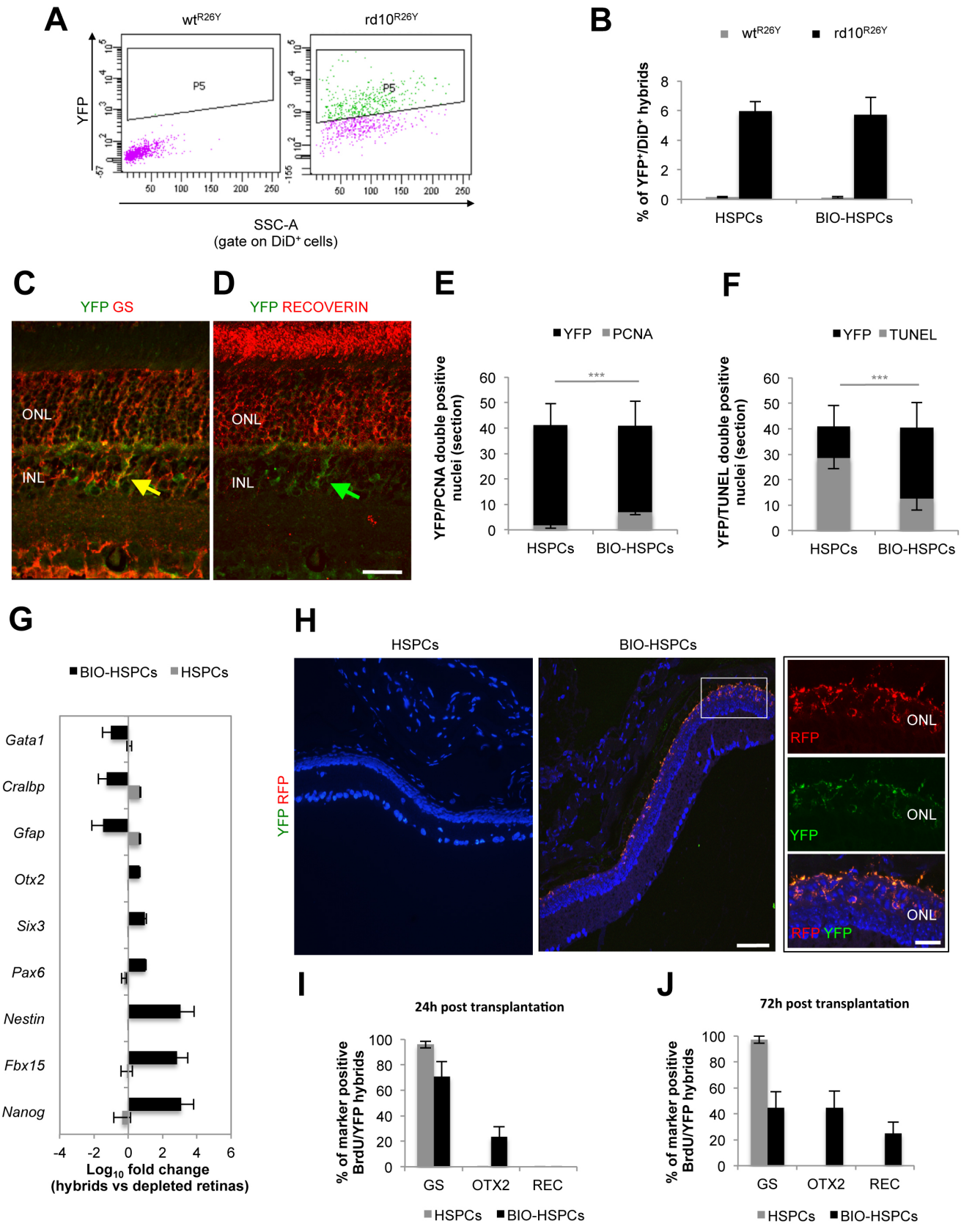
A
wtR26Y
rd10R26Y
YFP
P5
SSC-A
(gate on DiD+ cells)
B
wtR26Y
rd10R26Y
% of YFP+/DiD+ hybrids
HSPCs
BIO-HSPCs
C
YFP GS
ONL
INL
D
YFP RECOVERIN
ONL
INL
E
YFP
PCNA
YFP/PCNA double positive nuclei (section)
***
HSPCs
BIO-HSPCs
F
YFP
TUNEL
YFP/TUNEL double positive nuclei (section)
***
HSPCs
BIO-HSPCs
G
BIO-HSPCs
HSPCs
Gata1
Cralbp
Gfap
Otx2
Six3
Pax6
Nestin
Fbx15
Nanog
Log10 fold change
(hybrids vs depleted retinas)
H
HSPCs
BIO-HSPCs
YFP RFP
RFP
ONL
YFP
ONL
RFP YFP
ONL
I
24h post transplantation
% of marker positive BrdU/YFP hybrids
GS
OTX2
REC
HSPCs
BIO-HSPCs
J
72h post transplantation
% of marker positive BrdU/YFP hybrids
GS
OTX2
REC
HSPCs
BIO-HSPCs

Figure S5. Wnt-dependent cell-fusion-mediated reprogramming of hybrids in *rd10* mice. (**A**) Representative FACS analysis of DiD^+/YFP^+ hybrids in the total DiD^+ population detected in P19 $rd10^{R26Y}$ (rd10/R26Y) or healthy R26Y (wt/R26Y) retinas harvested 24 h after transplantation of $HSPCs^{Vav\text{-}Cre}$. (n=3). (**B**) Statistical analysis of the percentages of double DiD^+/YFP^+ hybrids evaluated on the total amount of DiD^+ untreated (HSPCs) or BIO-treated (BIO-HSPCs) $HSPCs^{Vav\text{-}Cre}$ detected by FACS in transplanted $rd10^{R26Y}$ (R26Y/rd10) or healthy R26Y (R26Y) retinas. Data are means ±S.D. from 3 independent experiments (n=3). (**C**, **D**) Representative immunostaining of YFP^+ hybrids (green) also immunoreactive to MG marker (GS, red in C, yellow arrow) but not to RECOVERIN (red in D, green arrow) detected 24 h after transplantation of $HSPCs^{Vav\text{-}Cre}$ in P18 $rd10^{R26Y}$ retinas. ONL: outer nuclear layer. INL: inner nuclear layer. Scale bar: 20 μm. (n=3). (**E**, **F**) Statistical analysis of the percentages of either proliferating ($PCNA^+$, E) or apoptotic ($TUNEL^+$, F) YFP^+ hybrids on the total amount of YFP^+ hybrids detected in $rd10^{R26Y}$ retinas 24 h after transplantation of untreated (HSPCs) or BIO-treated (BIO-HSPCs) $HSPCs^{Vav\text{-}Cre}$. Bars represent means ±S.D. from 3 independent experiments (n=9). ***P-value by unpaired Students' t-test <0.0001. (**G**) RT-PCR analysis of gene expression levels in DiD^+/YFP^+ hybrids FACS sorted 24 h after transplantation of DiD-labeled untreated (HSPCs) or BIO-treated (BIO-HSPCs) $HSPCs^{Vav\text{-}Cre}$ in P18 $rd10^{R26Y}$ retinas. Data represent Log_{10} fold changes ±SEM calculated with respect to the DiD^+/YFP^+-depleted retinas from 3 independent experiments (n=3). (**H**) Representative immunostaining of YFP^+ (green) /RFP^+ (red) hybrids detected in $rd10^{R26Y}$ retinas 42 days after transplantation of untreated (HSPCs) or BIO-treated (BIO-HSPCs) $HSPCs^{Vav\text{-}Cre/RFP}$. Scale bar: 200 μm. Right panels represent the single channel separation of a zoom of the retina transplanted with BIO-treated HSPCs (BIO-HSPCs) in the region where hybrids were detected (white square). Nuclei were counterstained with DAPI (blue). ONL: outer nuclear layer. Scale bar in right panel: 20 μm. (**I, J**) Statistical analysis of the percentage of double $YFP^+/BrdU^+$ hybrids also positive for GS, OTX2 or RECOVERIN stainings 24 h (I) or 72 h (J) after tranplantation of untreated (HSPCs, gray bars) or BIO treated (BIO-HSPCs, black bars) $HSPCs^{Vav\text{-}Cre}$ in P18 $rd10^{R26Y}$ retinas. Bars are means ±S.D. from 3 independent experiments (n=9). ***P-value by unpaired Students' t-test <0.0001.

Figure S6

A

MOUSE ID	OCT	MAX ONL ROWS OD	MAX ONL ROWS OS	MAX INL ROWS OD	MAX INL ROWS OS	MAX GC NUCLEI OD	MAX GC NUCLEI OS
#412	+	6	3	5	6	38	41
#413	+	4	2	6	7	38	36
#414	+	6	2	7	7	37	38
#416	+	6	2	7	7	40	41
#421	+	6	3	5	5	41	41
#422	+	6	2	5	5	39	38
#444	+	4	2	6	5	38	39
#445	+	5	2	6	5	41	40
#446	+	4	2	4	4	42	41
#408	-	2	1	6	6	39	38
#409	-	2	2	6	5	38	39
#410	-	2	1	5	4	39	40
#411	-	2	2	4	5	40	39
#415	-	3	2	7	5	41	40
#417	-	1	2	5	5	40	39
#419	-	2	2	5	5	39	40
#434	-	2	2	5	5	30	31
#435	-	2	2	6	5	41	40
#436	-	2	2	6	6	42	41
#437	-	2	2	5	5	39	40
#438	-	2	1	5	6	42	41
#439	-	1	1	5	5	41	43
#440	-	2	2	4	5	39	40
#441	-	2	2	5	5	40	39
#442	-	2	1	4	4	42	41
#443	-	1	2	4	5	42	41
#447	-	2	2	4	4	39	40
#449	-	1	1	5	4	38	38

B

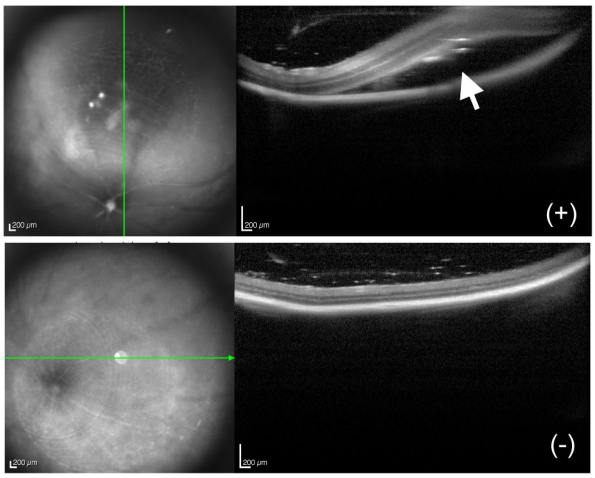

C

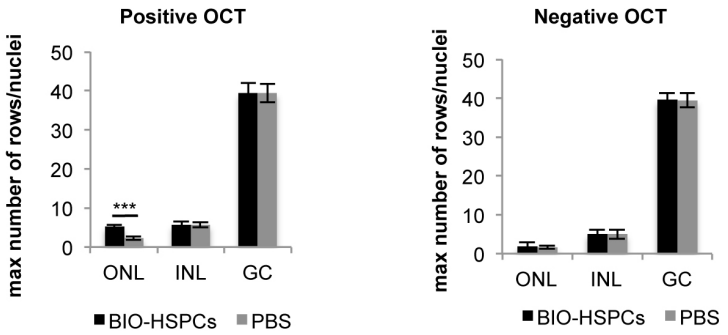

D

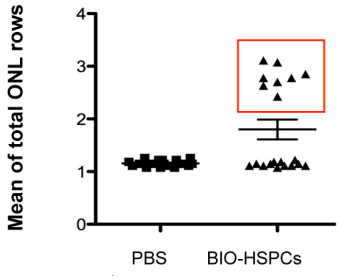

E

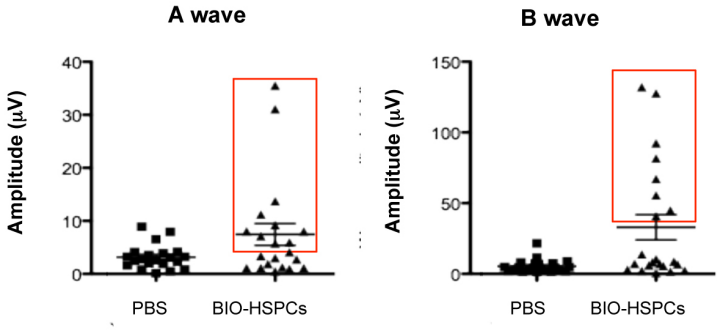

F

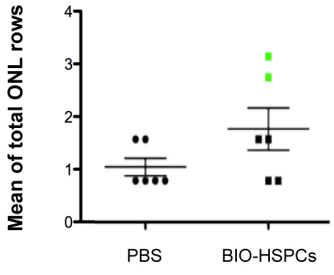

G

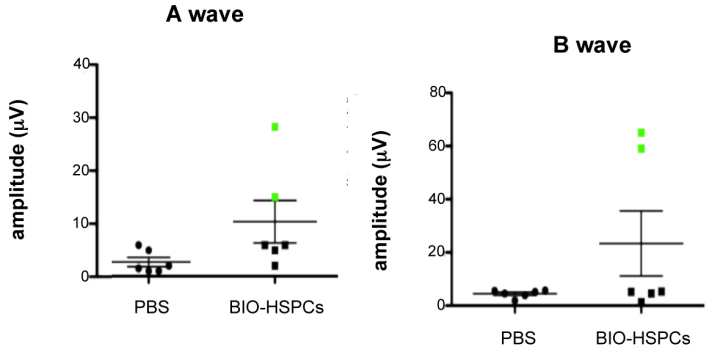

Figure S6. Analysing the correct delivery of cells after sub-retinal transplantation.
(**A-C**) Correlation of the correct delivery of the cells with the maximum number of either ONL or INL nuclear rows or the number of ganglion cell nuclei counted in P60 *rd10* right eyes (OD) transplanted with BIO-treated HSPCs or in left eyes (OS) treated with PBS as control. (**A**) After optical coherence tomography (OCT) analysis the detection of the retinal detachment was associated with a positive (+) score for the correct delivery of HSPCs in the sub-retinal space. A negative (-) score was attributed to mice where the retinal detachment was not observed. The maximum number of either ONL or INL nuclear rows detected in 3 different regions for 9 retinal sections for each eye was evaluated 42 days after cell transplantation by histological analysis. All the mice in which cells were correctly injected in the subretinal space (scored + at the OCT) were also found positive for regeneration. (n=28). (**B**) Representative images of the OCT analysis performed soon after cell transplantation from mice scored as positive (+) or negative (-) for the correct delivery of cells in the sub-retinal space assessed through the detection of a retinal detachment (arrow) in correspondence to the injection site (temporal area). The retinal detachment is also visible from the analysis of the ocular fundus (white line). Green lines indicate the position of the stack chosen for the vertical images. (n=28). (**C**) Statistical analysis of the maximum number of the nuclear rows detected in either the ONL or the INL and of the maximum number of ganglion nuclei counted in P60 *rd10* right eyes (OD) transplanted with BIO-treated HSPCs or in left eyes (OS) treated with PBS as control. Values are means ± S.D. (Positive OCT: n=9; Negative OCT: n=19). ***P-value by unpaired Students' t-test <0.0001. (**D**) Distribution of the mean of the ONL nuclear rows counted in 3 different regions for 9 different retinal serial sections for both right BIO-HSPCs transplanted and left PBS-treated eyes of each mouse (n=21). (**E**) Amplitudes of A-wave (A wave) and B-wave (B wave) recorded by ERG from either right *rd10* eyes transplanted with BIO-treated HSPCs (BIO-HSPCs) or left eyes treated with vehicle alone (PBS), 42 days after treatment (n=21). A group of retinas included in the red squares were positive to both the histology analysis (**D**) and the ERG (**E**)**.** (**F**) Distribution of the mean of ONL nuclear rows counted in 3 different regions for 9 different retinal serial sections for each $rd10^{R26Y}$ mouse (n=6), 42 days after BIO-treated (BIO-HSPCs) $HSPCs^{Vav\text{-}Cre}$ transplantation. (**G**) Amplitudes of A-wave (A wave) and B-wave (B wave) of the ERG scotopic response from either dark-adapted $rd10^{R26Y}$ eyes transplanted with BIO-treated (BIO-HSPCs) $HSPCs^{Vav\text{-}Cre/RFP}$ or treated with vehicle alone (PBS) as control, 42 days after treatment (n=6). (**F, G**) Green dots highlight retinas in which YFP^{+} hybrids were detected (shown in S5H) and that were positive to both the histology (**F**) and the ERG (**G**) analysis.

Table S1. List of the oligos used for RT-PCR analysis.

Oct4	fw CGTGGAGACTTTGCAGCCTG	rv GCTTGGCAAACTGTTCTAGCTCCT
Nanog	fw GCGCATTTTAGCACCCCACA	rv GTTCTAAGTCCTAGGTTTGC
Fbx15	fw ATGAGCTAGTGGCCGGGCC	rv TGTTGGTCAGTGTTGGGGAGTCG
Nestin	fw TGGAAGTGGCTACA	rv TCAGCTTGGGGTCAGG
Six3	fw GTGGACGGCGACTCTGC	rv CAACTGGTTTAAGAACCGGC
Six6	rv CAGGCAACCGGACTGACC	rv ACCTGCTGCTGGAGTCTGTT
Pax6	fw CCACCCATGCCCAGCTT	rv AACTGACACTCCAGGTGAAATGAG
Otx2	fw ACCCCTCCGTGGGCTACCC	rv CAGTGCCACCTCCTCAGGC
Crx	fw CATCCCCGAGACCCTCTACA	rv GGCTGGACTCAAATGGACA
Nrl	fw CCTCTATAAGGCCCGCTGTG	rv AGGCTCAGAGGAAGAGGTGT
Gfap	fw GGAGACGCATCACCTCTGCGC	rv AGAAATCCACCCGGGTCGGG
Cralbp	fw CAAGAGGCAGTATTCAGAC	rv GAAGAGTTCAGGGTACTGG
Rds	fw CGGGACTGGTTCGAGATTC	rv ATCCACGTTGCTCTTGATGC
Rho	fw GCTGTAATCTCGAGGGCTTC	rv CACCCATGATAGCGTGATTC
Opn1mw	fw GGCAATGTGAGATTTGATGC	rv CAGTACCTGCTCCAACCAAA
Opn1sw	fw TTCCCTCATCTGCTTCTCCT	rv TATGACTCACCTCCCGTTCA
Calr	fw AGCTGTAGAGGCCACACCACC	rv TGGAGAAAGGGAGGGACAGAAGG
Brn3a	fw TTGACCAGAGACACTTAC	rv TTTGGTGATGGTTGGTAG
Brn3b	fw CTGAGCCCAAATCAGAGAGATTGTGAAC	rv GCCGAGCAGCCCAGGTGC
PKCa	fw TTCAAGCCCAAAGTGTGTGG	rv GGGGTTGACATACGAGAACCC
Axin2	fw GGGAGCAGTTTTGTGGCAGCA	rv AGGGTCCTGGGTAAATGGGTGAG
Gapdh	fw GTATGACTCCACTCACGGCAAA	rv TTCCCATTCTCGGCCTTG

SUPPLEMENTARY REFERENCE

63. Meijer L, Flajolet M, and Greengard P. Pharmacological inhibitors of glycogen synthase kinase 3. *Trends Pharmacol Sci.* 2004;25(9):471-80.